Syntheses and X-ray structures of boraamidinate complexes of lithium, phosphorus, and tellurium

Tristram Chivers, Chantall Fedorchuk, Gabriele Schatte, and Justin K. Brask

Abstract: The dilithiated boraamidinate complexes $\{Li_2[RB(N\text{-}t\text{-}Bu)_2]\}_2$ (**1a**, R = Ph; **1b**, R = *t*-Bu), prepared by the reaction of B[N(H)-*t*-Bu]$_3$ with three equivalents of LiR, are shown by X-ray crystallography to have dimeric structures consisting of a distorted Li_4N_4 cube capped on two opposite faces by RB units. Reactions of **1a** with $TeCl_4$ or PX_3 (X = Cl, Br) yielded complexes PhB(μ-N-*t*-Bu)$_2$TeCl$_2$ (**2**) and PhB(μ-N-*t*-Bu)$_2$PX (**4a**, X = Cl; **4b**, X = Br), respectively. The structures of **2** and **4b** were determined by X-ray crystallography. In the solid state, complex **2** forms a dimer with weak Te···Cl contacts (3.2411(6) Å). Complex **4b** is monomeric with a P—Br bond length of 2.3047(11) Å. The reactions of **2** and **4a** with the appropriate amounts of Li[N(H)-*t*-Bu] produce the monomeric tellurium imide PhB(μ-N-*t*-Bu)$_2$Te=N-*t*-Bu and the amido derivative PhB(μ-N-*t*-Bu)$_2$PN(H)-*t*-Bu (**4c**), respectively. The X-ray structure of **4c** was determined. Deprotonation of **4c** with *n*-BuLi produces the dimeric monolithium derivative {Li[PhB(μ-N-*t*-Bu)$_2$PN-*t*-Bu]}$_2$ (**5**), which was shown by X-ray crystallography to have a centrosymmetric structure with a central transoid Li_2N_2 ring.

Key words: boraamidinates, lithium, tellurium, phosphorus, X-ray structures.

Résumé : Faisant appel à la diffraction des rayons X, on a montré que les structures des complexes boraamidinates dilithiés $\{Li_2[RB(N\text{-}t\text{-}Bu)_2]\}_2$ (**1a**, R = Ph; **1b**, R = *t*-Bu) préparés par réaction du B[N(H)-*t*-Bu]$_3$ avec trois équivalents de LiR sont des dimères formés d'un cube Li_4N_4 déformé et portant des unités RB sur deux faces opposées. Les réactions de métathèse du composé **1a** avec le $TeCl_4$ ou le PX_3 (X = Cl, Br) fournissent respectivement les complexes PhB(μ-N-*t*-Bu)$_2$TeCl$_2$ (**2**) et PhB(μ-N-*t*-Bu)$_2$PX (**4a**, X Cl; **4b**, X = Br). Les structures des composés **2** et **4b** ont été déterminées par diffraction des rayons X. Le complexe **2** forme un dimère avec de faibles contacts Te···Cl (3,2411(6) Å) à l'état solide. Le complexe **4b** est un monomère dans lequel la longueur de la liaison P—Br est de 2,3047(11) Å. Les réactions des composés **2** et **4a** avec des quantités appropriées de Li[N(H)N-*t*-Bu)] conduisent à la formation respectivement de l'imide de tellure monomère PhB(μ-N-*t*-Bu)$_2$Te=N-*t*-Bu et du dérivé amido PhB(μ-N-*t*-Bu)$_2$PN(H)-*t*-Bu (**4c**). On a déterminé la structure du composé **4c** par diffraction des rayons X. La déprotonation du composé **4c** à l'aide de *n*-BuLi conduit à la formation du dérivé monolithié dimère {Li[PhB(μ-N-*t*-Bu)$_2$PN-*t*-Bu]}$_2$ (**5**) dont structure, telle que déterminé par diffraction des rayons X, est centrosymétrique avec un cycle central Li_2N_2 transoïde.

Mots clés : boraamidates, lithium, tellure, phosphore, structures par diffraction des rayons X.

[Traduit par la Rédaction]

Introduction

Amidinate ligands $(RC(NR')_2)^-$ (**A**) have been investigated extensively as ligands for *p*- and *d*-block metals (1). Recent studies have focused on the application of aluminum (2) and early transition-metal (3) complexes as catalysts for alkene polymerization. By contrast, the isoelectronic boraamidinate dianions $(RB(NR')_2)^{2-}$ (**B**) have received restricted attention. The known complexes of **B** are limited almost exclusively to elements from groups 4, 14, or 16 (4).

The most straightforward route to such complexes involves metathesis between a halide and the reagent $\{Li_2[PhB(N\text{-}t\text{-}Bu)_2]\}_2$, prepared in situ by dilithiation of PhB[N(H)-*t*-Bu]$_2$ with *n*-BuLi (5). This method has been used for the synthesis of complexes of the type PhB(μ-N-*t*-Bu)$_2$ML$_n$ (where ML$_n$ = Pb(II) (5), ZrCp$_2$ (6), and SnMe$_2$ (6)) as well as the spirocyclic compounds [PhB(μ-N-*t*-Bu)$_2$]$_2$M (where M = Ge, Sn, Ti, or Zr (6), Te (7)). The fluorinated compound C_6F_5B(μ-N-*t*-Bu)$_2$SnMe$_2$ has been obtained in a similar manner (8). Less direct methods have been employed for the synthesis of the following boraamidinates: [MeB(μ-NSiMe$_3$)$_2$Sn]$_2$ (9), *t*-BuB(μ-N-*t*-Bu)$_2$P(N-*t*-Bu)-*t*-Bu (10), RB(μ-NR′)$_2$S (R = alkyl, aryl, C_6F_5; R′ = *t*-Bu or SiMe$_3$) (11), MeB[μ-N(2,6-Me$_2$CH)$_2$C$_6$H$_3$]$_2$SiMe$_2$ (12), MesB(μ-N-*t*-Bu)$_2$Si(SiMe$_3$)(Mes) (13), and PhB(μ-N-*t*-Bu)$_2$TeN-*t*-Bu (14).

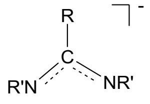

A

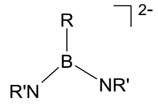

B

More recently, we have reported an alternative and potentially more versatile route to boraamidinates that involves the reaction of B(NH-*t*-Bu)$_3$ with three equivalents of an

Received 3 April 2002. Published on the NRC Research Press Web site at http://canjchem.nrc.ca on 26 June 2002.

T. Chivers,[1] C. Fedorchuk, G. Schatte, and J.K. Brask. Department of Chemistry, University of Calgary, Calgary, AB T2N 1N4, Canada.

[1] Corresponding author (e-mail: chivers@ucalgary.ca).

DOI: 10.1139/V02-111

alkyl-lithium reagent (15). The dilithium salts $\{Li_2[RB(N\text{-}t\text{-}Bu)_2]\}_x$ obtained in this way form either dimeric (R = *n*-Bu; *x* = 2, **1c**) or trimeric (R = Me; *x* = 3) clusters (15). In this article we describe (*i*) the synthesis and X-ray structures of $\{Li_2[RB(N\text{-}t\text{-}Bu)_2]\}_2$ (R = Ph, *t*-Bu); (*ii*) the preparation and X-ray structure of $PhB(\mu\text{-}N\text{-}t\text{-}Bu)_2TeCl_2$ and a new route to the monomeric tellurium imide $PhB(\mu\text{-}N\text{-}t\text{-}Bu)_2TeN\text{-}t\text{-}Bu$; and (*iii*) the preparation, spectroscopic characterization, and X-ray structure (X = Br) of the P(III) boraamidinates $PhB(\mu\text{-}N\text{-}t\text{-}Bu)_2PX$ (X = Cl, Br, N(H)-*t*-Bu), and the dimeric lithium derivative $\{Li[PhB(\mu\text{-}N\text{-}t\text{-}Bu)_2PN\text{-}t\text{-}Bu]\}_2$.

Experimental

Reagents and general procedures

The compounds $PhBCl_2$ (Aldrich, 97%), PCl_3 (Aldrich, 98%), PBr_3 (Aldrich, 99.99+%), and $TeCl_4$ (Alfa Aesar, 99.9%) were used as received. Li[N(H)-*t*-Bu] was prepared by the addition of *n*-BuLi (2.5 M solution in hexanes, 200 mL, 0.5 mol; Aldrich) to a solution of anhydrous *t*-$BuNH_2$ (65 mL, 0.609 mol; Aldrich, 98%) in *n*-hexane (170 mL) at –10°C and its purity was checked by ^1H NMR spectroscopy (δ in C_7D_8, 1.37 (*t*-Bu) and in THF-d_8, 1.07 (*t*-Bu), –1.55 (NH)). The compound $\{Li_2[n\text{-}BuB(N\text{-}t\text{-}Bu)_2]\}_2$ (**1c**) (15) was obtained in 70% yield from the reaction of $B[N(H)\text{-}t\text{-}Bu]_3$ (16) with three equivalents of *n*-BuLi. Solvents were dried with appropriate drying agents and distilled onto molecular sieves before use. All reactions and the manipulation of moisture-sensitive products were carried out under an atmosphere of argon or under vacuum. All glassware was carefully dried prior to use.

Instrumentation

^1H NMR spectra were recorded on Bruker AC 200 and DRX 400 spectrometers, and chemical shifts are reported relative to Me_4Si in $CDCl_3$. ^{13}C, ^{11}B, ^{31}P, ^{125}Te, and ^7Li NMR spectra were measured at 23°C in C_6D_6, $CDCl_3$, or C_4D_8O on a Bruker DRX 400 spectrometer using a 5-mm broadband probe operating at 100.613, 128.377, 161.975, 126.429, and 155.505 MHz, respectively. The samples were externally referenced to $BF_3{\cdot}Et_2O$ in C_6D_6, H_3PO_4 in D_2O, K_2TeO_3 in D_2O (referenced to Me_2Te), and 1.0 M LiCl in D_2O, respectively. Line-broadening parameters, used in the exponential multiplication of the free induction decays, were 50–0.5 Hz. Chemical shifts with a positive sign are correlated with shifts to high frequencies (downfield) of the reference compound. EPR spectra were recorded at 20°C on a Buker EMX 10/12 EPR spectrometer equipped with a microwave X-Band bridge (9.1–9.9 GHz), a 10-inch magnet, and a 12-kW power supply ER083CS. Samples of **1a** and **1c** were loaded into a 4-mm glass tube in a glovebox and dissolved in oxygen-free toluene. After brief exposure of these solutions to dry air, the EPR spectra were recorded. Mass spectra were obtained with a VG Micromass spectrometer VG7070 (70 eV). Infrared spectra were obtained as Nujol mulls between KBr plates on a Nicolet Nexus 470 FT-IR spectrometer in the range of 4000–350 cm^{-1}. Elemental analyses were provided by the Analytical Services Laboratory of the Department of Chemistry, University of Calgary.

Preparation of $\{Li_2[PhB(N\text{-}t\text{-}Bu)_2]\}_2$ (1a)

From $B[N(H)\text{-}t\text{-}Bu]_3$ and 3 equivalents of LiPh

A solution of LiPh in cyclohexane–ether (1.8 M, 3.70 mL, 6.67 mmol) was added slowly to a solution of $B[N(H)\text{-}t\text{-}Bu]_3$ (0.50 g, 2.22 mmol) in Et_2O (50 mL) at 23°C and the mixture was stirred for 18 h. Concentration by removal of solvent in vacuo, and subsequent cooling (0°C for 18 h) of the resulting yellow solution (~20 mL) yielded colourless hexagonal blocks of $\{Li_2[PhB(N\text{-}t\text{-}Bu)_2]\}_2$ (0.82 g, 1.69 mmol, 76%); mp. 158–160°C (dec.). ^1H NMR (C_6D_6) δ: 7.38–7.18 (m, 5H, C_6H_5), 1.09 (s, 18H, C_4H_9). ^{13}C NMR (C_6D_6) δ: 133.85, 126.41, 125.12 (C_6H_5), 51.52 (CMe_3), 35.33 (CMe_3). ^{11}B NMR (C_6D_6) δ: 35.4 (br). ^7Li NMR (C_6D_6) δ: +2.24 (s). Anal. calcd. for $C_{28}H_{46}B_2Li_4N_4$: C 68.90, H 9.50, N 11.48; found: C 67.76, H 9.50, N 10.47.

A 1-mL aliquot of the initial Et_2O reaction mixture was pumped to dryness in vacuo and taken up in C_6D_6. The ^1H and ^7Li NMR spectra indicated the presence of Li[N(H)-*t*-Bu]: ^1H NMR δ: 1.36 (s, C_4H_9), cf. lit.: 1.37 (17). ^7Li NMR δ: 0.14 (s).

From $PhB[N(H)\text{-}t\text{-}Bu]_2$ and two equivalents of n-BuLi

$PhB[N(H)\text{-}t\text{-}Bu]_2$ is obtained by adding a solution of $PhBCl_2$ (2.000 g, 64 mL, 12.54 mmol) in *n*-hexane (20 mL) to a slurry of Li[N(H)-*t*-Bu] (3.900 g, 49.32 mmol)[2] in *n*-hexane (30 mL) at –20°C. The reaction mixture was stirred for 4 h at 23°C and then filtered twice using a glass-sintered frit (8 μm) and then a PTFE filter disk (Acrodisc syringe filter; diameter: 25 mm; pore size: 0.45 μm). The volatile materials were removed under vacuum to give $PhB[N(H)\text{-}t\text{-}Bu]_2$ as a golden yellow oil (2.600 g, 11.20 mmol, 89%). IR (cm^{-1}): 3429 (NH). ^1H NMR (C_6D_6) δ: 7.54–7.17 (m, 5H, C_6H_5), 2.80 (br s, 2H, NH), 1.12 (s, 18H, C_4H_9). ^{13}C NMR (C_6D_6) δ: 133.12, 127.81, 127.61 (C_6H_5), 49.32 (CMe_3), 33.63 (CMe_3). ^{11}B NMR (C_6D_6) δ: 29.6.

The product was dissolved in *n*-hexane (20 mL) and the solution was cooled to –10°C. Then *n*-BuLi in hexane (2.5 M, 9 mL, 22.20 mmol) was added, and the reaction mixture was heated at reflux for 17 h. The white precipitate of **1a** was allowed to settle and the yellow solution was removed via a cannula and discarded. The product was washed twice with *n*-hexane (~5 mL) at 0°C giving **1a** (2.220 g, 4.55 mmol, 81%). The ^1H, ^{13}C, and ^{11}B NMR spectral parameters were in good agreement with those obtained for **1a** prepared by method A.

An increase in the scale of the reaction of $PhBCl_2$ with Li[N(H)-*t*-Bu] by a factor of two results in lower yields (60–80%) of $PhB[N(H)\text{-}t\text{-}Bu]_2$.

Preparation of $\{Li_2[t\text{-}BuB(N\text{-}t\text{-}Bu)_2]\}_2$ (1b)

tert-Butyllithium (3.30 mL, 5.61 mmol) was added slowly to a solution of $B[N(H)\text{-}t\text{-}Bu]_3$ (0.425 g, 1.87 mmol) in *n*-pentane (10 mL) at 23°C and stirred for 2.5 h. Concentration by removal of solvent in vacuo and subsequent cooling (0°C

---

[2] It is necessary to use an excess of Li[N(H)-*t*-Bu] to optimize the yield of $PhB[N(H)\text{-}t\text{-}Bu]_2$. Unreacted Li[N(H)-*t*-Bu] is readily removed by filtration.

for 3 h) of the resulting solution (~2 mL) yielded colourless rods of **1b** (0.342 g, 0.76 mmol, 81%). ^{1}H NMR (C_6D_6) δ: 1.48 (s, 9H, BC_4H_9), 1.38 (s, 18H, NC_4H_9). ^{7}Li NMR (C_6D_6) δ: –0.55 (s). ^{11}B NMR (C_6D_6) δ: 35.1 (s). Anal. calcd. for $C_{12}H_{27}BLi_2N_2$: C 64.33, H 12.15, N, 12.50; found: C 64.70, H 11.32, N 12.58.

Preparation of PhB(μ-N-*t*-Bu)$_2$TeCl$_2$ (2)

The addition of a colourless solution of **1a** (1.000 g, 2.049 mmol) in toluene (10 mL) to a yellow solution of $TeCl_4$ (1.104 g, 4.098 mmol) in toluene (15 mL) at –78°C produced a dark red solution, which became black upon warming to 23°C. After 1 h, the volatiles were removed under vacuum and the solid black residue was extracted with acetonitrile (2 × 10 mL). Elemental tellurium (50 mg) was separated by filtration through an Acrodisc syringe filter (PTFE membrane, pore size 0.45 μm) to give an orange solution. Removal of solvent under vacuum produced PhB(μ-N-*t*-Bu)$_2$TeCl$_2$ (1.604 g, 3.742 mmol, 91%) as an orange-yellow solid; mp 110–114°C dec. ^{1}H NMR (C_6D_6) δ: 7.51–7.16 (m, 5H, C_6H_5), 1.22 (s, 18H, C_4H_9); ($CDCl_3$) δ: 7.60–7.38 (m), 1.29 (s). ^{13}C NMR (C_6D_6) δ: 131.08, 129.75, 128.49 (C_6H_5), 55.76 (*C*Me$_3$), 33.70 (C*Me*$_3$). ^{11}B NMR (C_6D_6) δ: 43.5; ($CDCl_3$) δ: 43.3. ^{125}Te NMR ($CDCl_3$) δ: 1677.1; (C_6D_6) δ: 1673.9. Anal. calcd. for $C_{14}H_{23}BCl_2N_2Te$: C 39.23, H 5.41, N 6.53; found: C 37.42, H 5.35, N 6.05.

Preparation of PhB(μ-N-*t*-Bu)$_2$TeN-*t*-Bu (3)

A slurry of Li[N(H)-*t*-Bu] (0.222 g, 2.800 mmol) in *n*-hexane (15 mL) was added to a yellow-orange solution of **2** (0.600 g, 1.400 mmol) in *n*-hexane (20 mL) cooled to –78°C. The reaction mixture was allowed to reach room temperature after 15 min, whereupon an orange solution containing a white solid (LiCl) was obtained. The mixture was stirred for 18 h, after which time the colour of the solution had changed to dark orange. The solution was filtered and the volatile materials were removed under vacuum to give a sticky red solid. Et_2O (5 mL) was added and at –60°C PhB(μ-N-*t*-Bu)$_2$TeN-*t*-Bu (**3**) crystallized from this solution. The red supernatant was removed via cannula, and the remaining yellow-brown solid was washed with Et_2O (2 × 5 mL) at –60°C to give **3** (0.233 g, 0.543 mmol, 39%). The final product was LiCl-free (^{7}Li NMR). ^{1}H NMR (C_6D_6) δ: 7.50–7.10 (m, 5H, C_6H_5), 1.71 (s, 9H, C_4H_9), 1.11 (s, 18H, C_4H_9); cf. lit. (14) δ: 7.6–7.2, 1.70, 1.11 (in C_6D_6). ^{13}C NMR (THF-d_8) δ: 132.03, 128.15, 128.00 (C_6H_5), 64.71 (*C*Me$_3$), 53.91 (*C*Me$_3$), 34.85 (C*Me*$_3$), 34.48 (C*Me*$_3$). ^{11}B NMR (THF-d_8) δ: 33.4 (br). ^{125}Te NMR (THF-d_8) δ: 1491.5 (s).

Preparation of PhB(μ-N-*t*-Bu)$_2$PCl (4a)

A colourless solution of **1a** (2.000 g, 4.098 mmol) in THF (15 mL) was added to a solution of PCl_3 (0.72 mL, 1.125 g, 8.195 mmol) in toluene (15 mL) at –78°C. The reaction mixture was allowed to reach room temperature after 0.5 h, whereupon a pale yellow solution containing a white solid (LiCl) was obtained. After 4 h, the reaction mixture was filtered through a PTFE filter disk (0.45 μm). The volatile materials were removed under vacuum to give a white solid. After addition of Et_2O (5 mL), the solution was filtered to remove LiCl. Further purification was achieved by sublimation at 100°C (10^{-3} torr) to give **4a** (2.028 g, 6.848 mmol, 84%) as a white solid; mp 104°C. ^{1}H NMR (C_6D_6) δ: 7.4–7.0 (m, 5H, C_6H_5), 1.15 (d, $^4J_{H,P}$ = 1.20 Hz, 18H, C_4H_9); (THF-d_8) δ: 7.44–7.30 and 7.13–7.08 (m, 5H, C_6H_5), 1.16 (d, $^4J_{H,P}$ = 0.96 Hz, 18H C_4H_9). ^{13}C NMR (THF-d_8) δ: 131.93, 129.54, 128.65 (3s, C_6H_5), 52.77 (d, $^2J_{C,P}$ = 6.10 Hz, *C*Me$_3$), 32.28 (d, $^3J_{C,P}$ = 6.90 Hz, C*Me*$_3$). ^{11}B NMR (THF-d_8) δ: 35.4 (s). ^{31}P NMR (THF-d_8) δ: 181.2 (s). MS *m*/*z*: 281 ([M – Me]$^+$), 225 ([M – N-*t*-Bu]$^+$). Anal. calcd. for $C_{14}H_{23}BClN_2P$: C 56.69, H 7.82, N 9.44; found: C 56.13, H 7.34, N 9.28.

Preparation of PhB(μ-N-*t*-Bu)$_2$PBr (4b)

A colourless solution of **1a** (0.500 g, 1.024 mmol) in THF (15 mL) was added to a solution of PBr_3 (0.195 mL, 0.555 g, 2.049 mmol) in toluene (10 mL) at –40°C. After 5 min, the reaction mixture was allowed to reach room temperature, whereupon a pale yellow solution containing a yellow-orange solid (LiBr) was obtained. The reaction mixture was filtered through a PTFE filter disk after 3.5 h. The volatile materials were removed under vacuum to give a pale sticky yellow solid. *n*-Hexane (~10 mL) was added and the cloudy solution was transferred into another Schlenk vessel leaving a microcrystalline yellow solid (0.293 g) (mainly LiBr). After removal of the solvent from the decanted solution an off-white, slightly sticky solid was recovered. The solid was identified as [PhB(μ-N-*t*-Bu)$_2$]PBr (**4b**, 0.600 g, 1.764 mmol, 86%) by multinuclear NMR spectroscopy and single crystal X-ray structure analysis. Two 20-mg samples of **4b** were dissolved in Et_2O and in a mixture of Et_2O–*n*-pentane (1:1) (~3 mL) in test tubes and colourless prism-like crystals were obtained from both samples after four days at –19°C. ^{1}H NMR (C_6D_6) δ: 7.6–7.2 (m, 5H, C_6H_5), 1.22 (d, $^4J_{H,P}$ = 1.00 Hz, 18H, C_4H_9); (THF-d_8) δ: 7.44 (m, 2H, C_6H_5), 7.34 (m, 3H, C_6H_5), 1.19 (d, $^4J_{H,P}$ = 1.12 Hz, 18H, C_4H_9). ^{13}C NMR (THF-d_8) δ: 131.88, 129.76, 128.62 (3s, C_6H_5), 53.21 (d, $^2J_{C,P}$ = 5.84 Hz, *C*Me$_3$), 32.07 (d, $^3J_{C,P}$ = 6.65 Hz, C*Me*$_3$). ^{11}B NMR (THF-d_8) δ: 34.5 (s). ^{31}P NMR (THF-d_8) δ: 199.5 (s). MS *m*/*z*: 340 (M$^+$), 325 ([M – Me]$^+$), 261 ([M – N-*t*-Bu]$^+$). Anal. calcd. for $C_{14}H_{23}BBrN_2P$: C 49.30, H 6.80, N 8.21; found: C 48.57, H 8.63, N 7.81.

Preparation of PhB(μ-N-*t*-Bu)$_2$P[N(H)-*t*-Bu] (4c)

A colourless solution of Li[N(H)-*t*-Bu] (0.133 g, 1.688 mmol) in THF (10 mL) was added to a solution of **4a** (0.500 g, 1.688 mmol) in THF (15 mL) at –20°C. The reaction mixture was allowed to reach room temperature after 10 min. The volatile materials were removed under vacuum after 4 h to give a white solid. *n*-Hexane (10 mL) was added and the resulting solution was filtered through a PTFE filter disk to remove LiCl. The solvent was removed under vacuum to give **4c** as a white solid (0.454 g, 1.362 mmol, 81%); mp 60°C. IR (cm^{-1}): 3347 (NH). ^{1}H NMR (C_7D_8) δ: 7.5–7.0 (m, 5H, C_6H_5), 2.37 (s, 1H, N*H*), 1.90 (d, $^4J_{H,P}$ = 0.90 Hz, 9H, C_4H_9), 1.25 (s, 18H, C_4H_9); (THF-d_8) δ: 7.36–7.30 and 7.27–7.20 (m, 5H, C_6H_5), 3.26 (d, $^2J_{H,P}$ = 6.0 Hz, 1H, N*H*), 1.31 (d, $^4J_{H,P}$ = 1.07 Hz, 9H, C_4H_9), 1.12 (s, 18H, C_4H_9). ^{13}C NMR (THF-d_8) δ: 132.09, 128.01, 127.96 (3s, C_6H_5), 51.74 (s, *C*Me$_3$), 51.67 (s, *C*Me$_3$), 33.27 (d, $^3J_{C,P}$ = 6.14 Hz, *C*Me$_3$), 33.03 (d, $^3J_{C,P}$ = 9.34 Hz, C*Me*$_3$). ^{11}B NMR (THF-d_8) δ: 32.66 (s). ^{31}P NMR (THF-d_8) δ: 94.02 (s). Anal.

calcd. for $C_{18}H_{33}BN_3P$: C 64.87, H 9.98, N 12.61; found: C 63.06, H 9.69, N 11.90.[3]

Preparation of $\{Li[PhB(\mu\text{-}N\text{-}t\text{-}Bu)_2N\text{-}t\text{-}Bu]\}_2$ (5)

A solution of *n*-BuLi (2.5 M, 0.60 mL, 1.50 mmol) in hexanes was added to a solution of **4c** (0.500 g, 1.50 mmol) in *n*-hexane (10 mL) at –78°C. After 2.5 h, the solvent was removed from the golden yellow solution under vacuum to give **5** as a white solid (0.443 g, 1.306 mmol, 87%); mp 151°C (dec.). The ^1H, ^{13}C, ^7Li, and ^{11}B NMR spectra of THF-d_8 solutions of this product at 23°C indicate the presence of two components (**5A** and **5B**) in the approximate molar ratio 3:1.

5A: ^1H NMR δ: 7.38–7.14 (m, 5H, C_6H_5), 1.24 (d, $^4J_{H,P}$ = 1.13 Hz, 9H, *exo*-C_4H_9), 1.13 (s, 18H, *endo*-C_4H_9). ^{13}C NMR δ: 127.59, 127.41, 127.21 (3s, C_6H_5), 53.09 (d, $^2J_{C,P}$ = 25.6 Hz, *exo*-CMe_3), 52.13 (d, $^2J_{C,P}$ = 7.7 Hz, *endo*-CMe_3), 36.47 (d, $^3J_{C,P}$ = 6.5 Hz, *exo*-CMe_3), 33.49 (d, $^3J_{C,P}$ = 6.5 Hz, *endo*-CMe_3). ^7Li NMR δ: 0.39 (s).[4] ^{11}B NMR δ: 31.68 (s). ^{31}P NMR δ: 129.89 (s).

5B: ^1H NMR δ: 7.38–7.14 (m, 5H, C_6H_5), 1.32 (s, 9H, *exo*-C_4H_9), 1.18 (s, 18H, *endo*-C_4H_9). ^{13}C NMR δ: 133.03, 132.49, 132.18 (3s, C_6H_5), 56.84 (d, $^2J_{C,P}$ = 18.7 Hz, *exo*-CMe_3), 51.58 (d, $^2J_{C,P}$ = 8.2 Hz, *endo*-CMe_3), 35.92 (d, $^3J_{C,P}$ = 10.9 Hz, *exo*-CMe_3), 33.38 (d, $^3J_{C,P}$ = 4.8 Hz, *endo*-CMe_3). ^{11}B NMR δ: 37.21 (s). ^{31}P NMR δ: 68.10 (s). X-ray quality crystals were obtained from a solution of this solid (0.040 g) in C_7D_8 after 5 days at –19°C in an NMR tube. Satisfactory CHN analyses could not be obtained because of the extremely moisture-sensitive crystalline samples of **5**.

X-ray analyses

Crystals suitable for X-ray diffraction were obtained from solutions of the desired compounds in *n*-pentane at 23°C (**1a**, **1b**), in $CDCl_3$ at 23°C (**2**), in Et_2O or Et_2O–*n*-pentane at –19°C (**4b**), in *n*-hexane at –19°C (**4c**), and in C_7D_8 at –19°C (**5**). Single crystals of **1a**, **1b**, **2, 4b**, **4c**, and **5** were coated with Paratone oil, mounted on thin glass fibres, and frozen in the cold nitrogen stream of the goniometer or on a CryoLoop (nylon fibre).

Measurements for **1a** and **1b** were made on a Bruker AXS SMART/Platform 1000 CCD (ω-scans) and on a Bruker AXS SMART/PY/RA/SMART 1000 CCD (ϕ- and ω-scans) diffractometer, respectively. The data were reduced with SAINT (18*a*), which corrects for Lorentz and polarization effects, and corrected for absorption with SADABS (18*b*).

X-ray data for **2**, **4b**, **4c**, and **5** were collected on a Nonius Kappa CCD 4-circle Kappa FR540C diffractometer using ϕ- and ω-scans. Data reduction was performed with the HKL, DENZO, and SCALEPACK (18*c*) software, which corrects for beam non-homogeneity, possible crystal decay, and *Lp* effects, respectively. A multiscan absorption correction was applied (SCALEPACK) (18*c*).

Relevant parameters for the data collections and crystallographic data for **1a**, **1b**, **2**, **4b**, **4c**, and **5** are summarized in Tables 1 and 2.[5]

All structures were solved using direct methods (**1a**, **1b**, **4b**: SHELXS-97 (19*a*); **4c**: SHELXS-97–2 (19*b*); **2**: SIR-92 (20*a*); **6**: SIR-97 (20*b*)) and refined by full-matrix least-squares methods on F^2 with SHELXL97–2 (19*b*). The non-hydrogen atoms were refined anisotropically. Hydrogen atoms were included at geometrically idealized positions (C—H and N—H bond distances 0.95 Å) and were not refined. The isotropic thermal parameters of the hydrogen atoms were fixed at 1.2 times that of the corresponding carbon or nitrogen atom.

Two of the carbon atoms (C(50) and C(53)) of the *t*-Bu group attached to B(1) in **1b** were disordered around the mirror plane with partial occupancy factors of 0.5 each, leading to two possible orientations of the disordered *t*-Bu group: C(52), C(50), C(51), C(53) and C(53)*, C(50)*, C(52), C(51) (*: *x*, –*y* + 1/2, *z*).

In **4b**, one of the carbon atoms (C(13), C(13)′) of one of the *t*-Bu groups was disordered around the mirror plane with partial occupancy factors of 0.62(2) and 0.38(2), respectively. In **4c**, the hydrogen atom connected to N(3) was located from the Fourier difference map.

Results and discussion

Synthesis and X-ray structures of $\{Li_2[RB(N\text{-}t\text{-}Bu)_2]\}_2$ (1a, R = Ph; 1b, R = *t*-Bu)

In a preliminary communication (15), we reported that the dilithio boraamidinate complexes $\{Li_2[RB(N\text{-}t\text{-}Bu)_2]\}_x$ (R = *n*-Bu, *x* = 2 (**1c**); R = Me, *x* = 2,3) were obtained by treatment of $B[N(H)\text{-}t\text{-}Bu]_3$ with three equivalents of the appropriate organolithium reagent. In this transformation the alkyl-lithium reagent functions as a base to dilithiate $B[N(H)\text{-}t\text{-}Bu]_3$ and as a nucleophile to displace the third *t*-BuNH group with an alkyl substituent.[6] Here we have demonstrated that aryl-lithium reagents can also be used in this new synthesis of boraamidinates. Thus $\{Li_2[PhB(N\text{-}t\text{-}Bu)_2]\}_2$ (**1a**) is obtained in 76% yield via eq. [1]. The preferred synthesis of **1a**, however, is the dilithiation of $PhB[N(H)\text{-}t\text{-}Bu]_2$, for which an improved procedure is described in the *Experimental* section (eq. [2]). The overall yield of **1a** from $PhBCl_2$ is ~73%; it is not necessary to separate the product from Li[N(H)-*t*-Bu] (cf. eq. [1]).

---

[3] Slightly low CHN values were obtained for three different samples. The product was, however, spectroscopically pure (^1H, ^{13}C, and ^{31}P NMR spectra) and showed no resonance for LiCl in the ^7Li NMR spectrum.

[4] Two very weak resonances were also observed in the ^7Li NMR spectrum at δ 1.07 and 1.60, but neither of these resonances were sufficiently intense to be attributable to **5B**. It is possible that the ^7Li NMR resonance for **5B** is hidden under the resonance at δ 0.39 for **5A**.

[5] Supplementary material may be purchased from the Depository of Unpublished Data, Document Delivery, CISTI, National Research Council Canada, Ottawa, ON K1A 0S2, Canada. For information on obtaining material electronically go to http://www.nrc.ca/cisti/irm/unpub_e.shtml. Crystallographic information has also been deposited with the Cambridge Crystallographic Data Centre (CCDC Nos. 181868 (**1a**), 181864 (**1b**), 181865 (**2**), 181866 (**4b**), 181867 (**4c**), and 181863 (**5**)). Copies of the data can be obtained free of charge via www.ccdc.cam.ac.uk/conts/retrieving.html (or from the Cambridge Crystallographic Data Centre, 12, Union Road, Cambridge CB2 1EZ, UK; fax: +44 1223 336033; or deposit@ccdc.cam.ac.uk).

[6] A similar transformation has been reported by Nöth et al. (21) for the lithiation of $MesP(NH\text{-}t\text{-}Bu)_2$ with *n*-BuLi, which produces $\{n\text{-}BuP[N(Li)\text{-}t\text{-}Bu]_2\}_2\cdot(OEt_2)_2$ via the nucleophilic substitution of the mesityl group at the phosphorus(III) centre by an *n*-butyl group.

Table 1. Crystallographic data for **1a**, **1b**, and **2**.

	1a	**1b**	**2**
Formula	$C_{24}H_{54}B_2Li_4N_4$	$C_{28}H_{46}B_2Li_4N_4$	$C_{14}H_{23}BCl_2N_2Te$
FW	448.09	488.07	428.65
Crystal size (mm)	0.39 × 0.30 × 0.13	0.48 × 0.21 × 0.15	0.30 × 0.30 × 0.25
Colour and habit	Colourless prism	Colourless prism	Orange plate
T (K)	193(2)	193(2)	173(2)
Wavelength (Å)	0.71073	0.71073	0.71073
Crystal system	Monoclinic	Monoclinic	Orthorhombic
Space group	$P2_1/m$	$C2/c$	$Pbca$
a (Å)	10.1301(11)	19.844(4)	14.8178(2)
b (Å)	11.0986(12)	8.9232(18)	11.5449(2)
c (Å)	13.4048(13)	17.876(4)	21.3800(3)
β (°)	100.8559(19)	100.970(3)	
V (Å^3)	1480.1(3)	3107.6(11)	3657.48(10)
Z	2	4	8
$D_{\text{calcd.}}$ (g cm^{-3})	1.005	1.043	1.557
μ (cm^{-1})	0.55	0.58	19.11
No. of reflns. collected	5783	7320	10310
No. of indep. reflns./R_{int}	2624/0.0446	3177/0.0529	5226/0.0196
Reflns. with $I > 2\sigma(I)$	1650	1784	4140
S (GoF) on F^2 [a]	1.025	0.923	1.021
R [$I \geq 2\sigma(I)$][b]	0.0571	0.0543	0.0265
wR (all data)[c]	0.1652	0.1452	0.0655
Largest diff. peak/hole (e Å^{-3})	0.188/–0.136	0.293/–0.220	0.625/–0.583

[a] $S = \{\Sigma[w(F_o^2 - F_c^2)^2]/(n - p)\}^{1/2}$.
[b] $R = \Sigma||F_o| - |F_c||/\Sigma|F_o|$.
[c] $wR = \{[\Sigma w(F_o^2 - F_c^2)^2]/[\Sigma w(F_o^2)^2]\}^{1/2}$.

Table 2. Crystallographic data for **4b**, **4c**, and **5**.

	4b	**4c**	**5**
Formula	$C_{14}H_{23}BBrN_2P$	$C_{18}H_{33}BN_3P$	$C_{36}H_{64}B_2Li_2N_4P_2$
FW	341.02	333.25	678.37
Crystal size (mm)	0.30 × 0.30 × 0.20	0.15 × 0.15 × 0.10	0.12 × 0.12 × 0.05
Colour and habit	Colourless prism	Colourless plate	Colourless plate
T (K)	223(2)	173(2)	173(2)
Wavelength (Å)	0.71073	0.71073	0.71073
Crystal system	Monoclinic	Monoclinic	Monoclinic
Space group	$P2_1/m$	$C2/c$	$P2_1/n$
a (Å)	6.2890(1)	36.1860(6)	11.2310(2)
b (Å)	13.8520(3)	6.0030(2)	10.4010(2)
c (Å)	10.0331(2)	25.2640(6)	18.4790(4)
β (°)	91.306(2)	131.0551(11)	107.2790(8)
V (Å^3)	873.80(3)	4138.35(18)	2061.18(7)
Z	2	8	2
$D_{\text{calcd.}}$ (g cm^{-3})	1.296	1.070	1.093
μ (cm^{-1})	24.33	1.36	1.37
No. of reflns. collected	4064	6619	9039
No. of indep. reflns./R_{int}	2423/0.0139	3507/0.0371	4695/0.0264
Reflns. with $I > 2\sigma(I)$	1785	2520	3703
S (GoF) on F^2 [a]	1.042	1.030	1.030
R [$I \geq 2\sigma(I)$][b]	0.0517	0.0381	0.0419
wR (all data)[c]	0.1442	0.0998	0.1146
Largest diff. peak/hole (e Å^{-3})	0.800/–0.949	0.210/–0.262	0.563/–0.382

[a] $S = \{\Sigma[w(F_o^2 - F_c^2)^2]/(n - p)\}^{1/2}$.
[b] $R = \Sigma||F_o| - |F_c||/\Sigma|F_o|$.
[c] $wR = \{[\Sigma w(F_o^2 - F_c^2)^2]/[\Sigma w(F_o^2)^2]\}^{1/2}$.

Table 3. Selected bond lengths and bond angles (deg) for **1a** and **1b**.

Bond lengths (Å)		Bond angles (deg)			
1a					
B(1)—N(1)	1.448(3)	B(1)-N(1)-Li(1)′	132.46(18)	Li(2)-N(2)-Li(1)	88.65(16)
B(1)—N(2)	1.449(3)	B(1)-N(1)-Li(1)	75.12(15)	Li(1)-N(2)-Li(2)′	68.34(15)
B(1)—C(31)	1.598(3)	B(1)-N(2)-Li(2)	78.15(16)	N(1)-B(1)-N(2)	109.50(18)
N(1)—Li(1)′	2.017(4)	B(1)-N(2)-Li(1)	75.93(16)	N(1)′-Li(1)-N(2)	110.64(18)
N(1)—Li(2)	2.027(4)	B(1)-N(1)-Li(2)	78.02(16)	N(1)′-Li(1)-N(1)	109.59(17)
N(1)—Li(1)	2.077(4)	B(1)-N(2)-Li(2)′	131.29(17)	N(2)-Li(1)-N(1)	69.93(14)
N(2)—Li(2)	2.022(4)	Li(1)′-N(1)-Li(2)	69.94(15)	N(2)-Li(2)-N(1)	71.52(13)
N(2)—Li(1)	2.052(4)	Li(1)′-N(1)-Li(1)	69.62(17)	N(2)-Li(2)-N(2)′	109.94(18)
N(2)—Li(2)′	2.074(4)	Li(2)-N(1)-Li(1)	87.84(16)	N(1)-Li(2)-N(2)′	109.34(18)
1b					
B(1)—N(1)	1.476(4)	N(1)-B(1)-N(2)	105.2(2)	Li(2)-N(3)-Li(3)	85.51(17)
B(1)—N(2)	1.479(4)	N(1)-B(1)-C(50)	126.6(3)	N(1)-Li(1)-N(2)	72.41(13)
B(1)—C(50)	1.660(5)	N(2)-B(1)-C(50)	126.4(3)	N(1)-Li(1)-N(3)	112.25(17)
B(2)—N(3)	1.476(2)	N(3)-B(2)-N(3)′	105.5(2)	N(2)-Li(1)-N(3)	111.41(17)
B(2)—C(60)	1.662(4)	N(3)-B(2)-C(60)	127.25(11)	N(1)-Li(2)-N(3)	111.22(19)
N(1)—Li(1)	1.980(4)	B(1)-N(1)-Li(1)	78.33(15)	N(3)-Li(2)-N(3)′	72.94(18)
N(1)—Li(2)	2.154(5)	B(1)-N(1)-Li(2)	132.1(2)	N(2)-Li(3)-N(3)	113.23(19)
N(2)—Li(1)	1.996(4)	Li(1)-N(1)-Li(2)	67.43(14)	N(3)-Li(3)-N(3)′	71.99(18)
N(2)—Li(3)	2.080(5)	B(2)-N(3)-Li(2)	79.65(15)	Li(1)-N(1)-Li(1)′	86.4(2)
N(3)—Li(1)	2.125(4)	B(2)-N(3)-Li(3)	76.36(16)	B(1)-N(2)-Li(1)	77.73(15)
N(3)—Li(2)	1.976(4)	B(2)-N(3)-Li(1)	131.94(15)	B(1)-N(2)-Li(3)	132.1(2)
N(3)—Li(3)	1.999(4)	Li(1)-N(3)-Li(2)	68.07(16)	Li(1)-N(2)-Li(3)	67.74(14)
		Li(1)-N(3)-Li(3)	66.79(15)	Li(1)-N(2)-Li(1)′	85.5(2)

Note: Symmetry transformations used to generate equivalent atoms ′: –*x* + 1/2, *y*, –*z*.

[1] $$\mathrm{B[N(H)\text{-}}t\mathrm{\text{-}Bu]_3 + 3LiPh \rightarrow 1/2\{Li_2[PhB(N\text{-}}t\mathrm{\text{-}Bu)_2]\}_2 + Li[N(H)\text{-}}t\mathrm{\text{-}Bu] + 2C_6H_6}$$

[2] $$\mathrm{PhBCl_2 + 2LiN(H)\text{-}}t\mathrm{\text{-}Bu \rightarrow PhB[N(H)\text{-}}t\mathrm{\text{-}Bu]_2 + 2LiCl \xrightarrow{2\mathit{n}\text{-}BuLi} 1/2\{Li_2[PhB(N\text{-}}t\mathrm{\text{-}Bu)_2]\}_2 + 2H\text{-}}n\mathrm{\text{-}Bu}$$

We have also shown that the *tert*-butyl derivative $\{\mathrm{Li_2}[t\text{-}\mathrm{BuB(N}\text{-}t\text{-}\mathrm{Bu)_2}]\}_2$ (**1b**) can be prepared in 81% yield by the reaction of B[N(H)-*t*-Bu]$_3$ with three equivalents of *t*-BuLi. It is interesting to compare this result with the related chemistry of transition-metal amides. The amido–niobium complex [(THF)$_2$Li]$_2$[Nb(NMes)$_3$(NHMes)] (Mes = 2,4,6-Me$_3$C$_6$H$_2$) is lithiated by *t*-BuLi to give the tetrakisimidoniobate (THF)$_4$Li$_3$[Nb(NMes)$_4$] (22*a*), whereas the reaction of the same complex with *n*-BuLi results in nucleophilic displacement of the amido ligand to give the alkyl–niobium complex [[(THF)$_2$Li]$_2$*n*-BuNb(NMes)$_3$] (22*b*).

Fig. 1. ORTEP drawing of $\{\mathrm{Li_2[PhB(N\text{-}}t\mathrm{\text{-}Bu)_2]}\}_2$ (**1a**) (30% probability ellipsoids). Primed atoms are related by the symmetry transformation: –*x* + 1/2, *y*, –*z*.

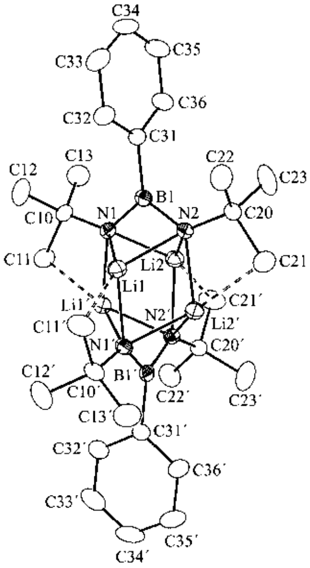

An intriguing observation, which was not reported in the earlier work (5, 6), is the appearance of persistent bright pink solutions when **1a**–**c** are exposed to air.[7] This transformation is reminiscent of the behaviour of solutions of the related dimeric clusters {Li$_2$[E(N-*t*-Bu)$_3$]}$_2$ (E = S, Se), which form deep blue (E = S) or green (E = Se) solutions upon air oxidation (23–25). These colours were attributed to the radicals $\{\mathrm{Li_3[E(N\text{-}}t\mathrm{\text{-}Bu)_3]_2}\}^{\bullet}$ on the basis of their EPR spectra, which consisted of a septet of decets with the appropriate relative intensities for the coupling of the unpaired electron with three nitrogen (^{14}N, 99.6%, *I* = 1) and three lithium (^{7}Li, 92.6%, *I* = 3/2) nuclei (24, 25). These neutral radicals are comprised of the radical anion $[\mathrm{E(N\text{-}}t\mathrm{\text{-}Bu)_3}]^{\bullet-}$ and the dianion $[\mathrm{E(N\text{-}}t\mathrm{\text{-}Bu)_3}]^{2-}$ bridged by three Li$^+$ ions. The pink solution of air-oxidized **1a** in toluene at 23°C exhibits a five-line EPR spectrum, but the hyperfine coupling with

---

[7] T. Chivers, C. Fedorchuk, G. Schatte, J.K. Brask, and R.T. Boeré. Unpublished results.

Table 4. Selected bond lengths (Å) and bond angles (deg) for **2**.

Bond lengths (Å)		Bond angles (deg)			
Te(1)—N(2)	1.9954(16)	Cl(2)-Te(1)···Cl(2)*	78.29(2)	B(1)-N(1)-C(10)	137.35(18)
Te(1)—N(1)	1.9998(16)	Cl(1)-Te(1)···Cl(2)*	94.53(2)	B(1)-N(1)-Te(1)	92.21(13)
Te(1)—Cl(1)	2.4356(6)	Cl(2)*-Te(1)-N(1)	168.06(2)	C(10)-N(1)-Te(1)	127.02(14)
Te(1)—Cl(2)	2.6452(6)	Cl(2)*-Te(1)-N(2)	108.97(2)	B(1)-N(2)-C(20)	136.69(18)
N(1)—B(1)	1.447(3)	Cl(1)-Te(1)-Cl(2)	172.73(2)	B(1)-N(2)-Te(1)	92.41(13)
N(2)—B(1)	1.447(3)	N(2)-Te(1)-N(1)	69.33(7)	C(20)-N(2)-Te(1)	129.46(14)
C(1)—B(1)	1.563(3)	N(2)-Te(1)-Cl(1)	94.48(5)	N(2)-B(1)-N(1)	103.49(19)
		N(1)-Te(1)-Cl(1)	97.38(5)	N(2)-B(1)-C(1)	127.08(18)
Te(1)···Cl(2)*	3.2411(6)	N(2)-Te(1)-Cl(2)	88.98(5)	N(1)-B(1)-C(1)	129.23(18)
		N(1)-Te(1)-Cl(2)	89.82(5)		

Note: Symmetry transformations used to generate equivalent atoms *: –*x*, –*y*, –*z*.

Scheme 1.

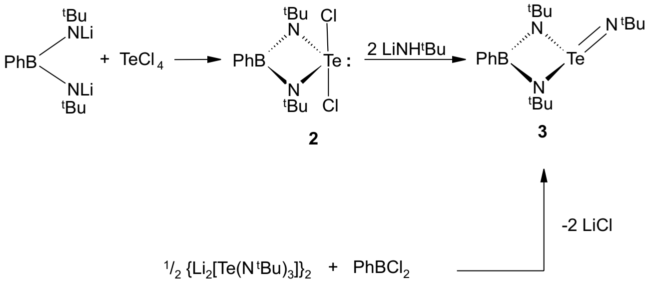

lithium centres is not resolved.[7] Consequently, we will not speculate on the identity of the radical species.

Because the structures of **1a** and **1b** were shown by X-ray crystallography to be similar, only the drawing of **1a** is shown (see Fig. 1). Pertinent structural parameters are compared in Table 3. The dimeric arrangement of **1a** and **1b** is similar to that previously reported for $\{Li_2[n\text{-BuB(N-}t\text{-Bu)}_2]\}_2$ (**1c**) (15); a detailed discussion here of the structures of **1a** and **1b** is therefore not warranted. All three structures consist of a distorted Li_4N_4 cube capped on two opposite faces by RB units, which are in a trigonal planar environment. Molecule **1b**, however, crystallizes in the space group $P2_1/m$ (cf. $P2_1/n$ for **1c**), imposing a mirror plane that bisects the cluster core at the atoms B(1), B(2), Li(2), Li(3), N(1), and N(2). Carbon atoms C(50) and C(53) of the *t*-Bu group attached to B(1) are disordered over two positions, each with site occupancy factors of 0.5. The replacement of the *n*-Bu groups attached to the boron atoms in **1c** with bulkier *t*-Bu groups results in lengthening of the B—N and B—C bonds (by ~0.02 and 0.05 Å, respectively) and contraction of the N-B-N angles (by ~3°). The weighted mean Li—N distance of 2.032 Å in **1b** is similar to that found for **1c** (2.037 Å), but the range of Li—N distances (1.976(4)–2.154(5) Å) is broader. The weighted mean distance of 2.226 Å for the agostic C–H···Li interactions in **1b** is significantly shorter (by ~0.2 Å) than that in **1c**, presumably as a result of the influence of the bulky *t*-Bu groups. Consistently, the mean C–H···Li contacts in**1a** (2.421 Å) are similar to the corresponding interaction exhibited by **1c** (2.440 Å).

Fig. 2. ORTEP drawing of $[PhB(\mu\text{-N-}t\text{-Bu})_2TeCl_2]_2$ (**2**) (30% probability ellipsoids). Starred atoms are related by the symmetry transformation: –*x*, –*y*, –*z*.

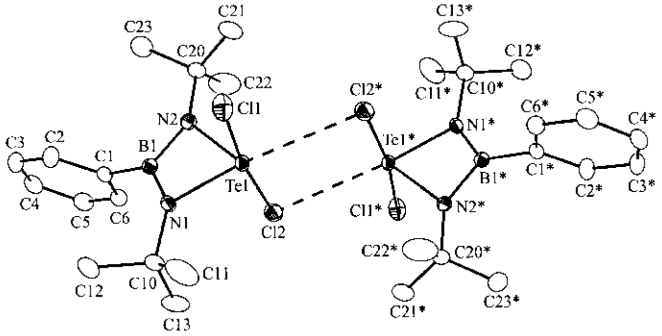

Phenylboraamidinate complexes of tellurium(IV)

We have shown earlier that a boraamidinate ligand stabilizes a monomeric tellurium imide in the complex $PhB(\mu\text{-N-}t\text{-Bu})_2Te\text{=N-}t\text{-Bu}$ (**3**) (14); however, the yield of this complex in the synthesis from $PhBCl_2$ and $\{Li_2[Te(N\text{-}t\text{-Bu})_3]\}_2$ was only 29%. Consequently, an alternative route to **3**, as depicted in Scheme 1, was investigated. The reaction of the monomer of **1a** with $TeCl_4$ in a 1:1 molar ratio produces $PhB(\mu\text{-N-}t\text{-Bu})_2TeCl_2$ (**2**) in 91% yield. The spirocyclic complex $[PhB(\mu\text{-N-}t\text{-Bu})_2]_2Te$ is obtained in 43% yield when a 2:1 stoichiometry is used for this reaction (7). Complex **2** was characterized by CHN analyses, multinuclear (^1H, ^{13}C, ^{11}B, and ^{125}Te) NMR spectroscopy,[8] and by an X-ray structural determination (vide infra). The subsequent reaction of **2** with two equivalents of Li[N(H)-*t*-Bu] produced **3** in ~40% yield. Although the improvement in the yield of **3** is modest, this new synthesis is preferable to the existing method using $\{Li_2[Te(N\text{-}t\text{-Bu})_3]\}_2$, (14) in view of the easier preparation of the reagents.

The structure of **2** was determined by X-ray crystallography (see Fig. 2). Selected bond lengths and bond angles are given in Table 4. Complex **2** forms a centrosymmetric dimer linked by weak Te···Cl interactions of 3.2411(6) Å (cf. sum of van der Waals radii for Te and Cl of 3.81 Å (27*a*) or 4.0 Å (27*b*)). Several bisamido or bisimido–tellurium dichloride complexes have been structurally characterized, including monomeric $[(Ph_3PN)_2TeCl_2$ (28), $(Ph_2CN)_2TeCl_2$ (29)],

---

[8] The ^{125}Te NMR resonance for **2** appears at δ 1677, which may be compared with the ^{125}Te chemical shifts of δ 1575 and 1693 observed for the inequivalent tellurium atoms in $t\text{-BuNTe}(\mu\text{-N-}t\text{-Bu})_2TeCl_2$ (26).

Fig. 3. ORTEP drawing of [PhB(μ-N-*t*-Bu)$_2$PBr] (**4b**) (30% probability ellipsoids).

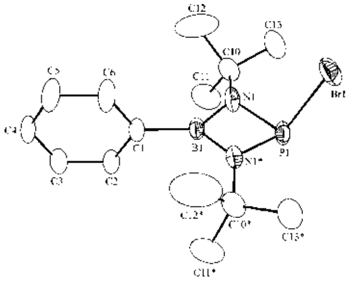

dimeric [(Me$_3$PN)$_2$TeCl$_2$ (30), CF$_3$SNTeCl$_2$·THF (31)], or extended structures [{Cl$_2$Te(μ-N-*t*-Bu)$_2$TeCl$_2$}$_3$ (26), [(Me$_3$Si)$_2$N]$_2$TeCl$_2$ (32), MeN[PhBN(Me)]$_2$TeCl$_2$ (7), (Ph$_2$SN)$_2$TeCl$_2$ (29), and *t*-BuN(H)Sb(μ-N-*t*-Bu)$_2$TeCl$_2$ (33)[9]]. The different degrees of oligomerization observed for closely related molecules suggest that packing considerations, influenced by subtle steric effects, are responsible for the presence (or absence) of association.

The boraamidinate ligand in **2** is symmetrically bonded to tellurium with equal B–N and Te–N bond lengths. The relevant bond angles (N(2)-Te(1)-N(1) = 69.33(7)°, Cl(2)*-Te(1)-N(1) = 168.06(2)°, Cl(2)*-Te(1)-N(2) = 108.97(2)°, Cl(1)-Te(1)-Cl(2) = 172.73(2)°) indicate that the tellurium atom in **2** is in a distorted pseudo-octahedral environment, with the lone pair occupying an octahedral site. The Te—N bond lengths (av 1.997 Å) can be compared with the values of 2.036 and 2.147 Å reported for the equatorial and axial bonds, respectively, in the spirocyclic compound [PhB(μ-N-*t*-Bu)$_2$]$_2$Te, which is a distorted trigonal bipyramid (7). The Te—Cl bond distances in **2** are significantly different (2.4356(6) and 2.6452(6) Å) as a result of the weak Te···Cl contacts, which are reflected by the non-linearity of the Cl-Te-Cl unit (172.73(2)°) and the Cl(2)-Te(1)···Cl(2)* bond angle (78.29(2)°) in the Te$_2$Cl$_2$ rectangle.

Phenylboraamidinate complexes of phosphorus(III)

We have also obtained boraamidinate complexes containing a phosphorus(III)–halogen bond in 85–95% yields by the reaction of **1a** with phosphorus trihalides (eq. [3]). The only previously reported P(III) complex is MeB(μ-N-*t*-Bu)$_2$PMe prepared by treatment of MeBBr$_2$ with (LiN-*t*-Bu)$_2$PMe (34). The complexes PhB(μ-N-*t*-Bu)$_2$PX (**4a**, X = Cl; **4b**, X = Br) were characterized by CHN analyses, multinuclear (^{1}H, ^{13}C, ^{11}B, and ^{31}P) NMR spectroscopy, mass spectrometry, and an X-ray structure determination of **4b**. The ^{1}H NMR spectra of **4a** or **4b** in C$_6$D$_6$ or THF-*d*$_8$ show resonances for the Ph and N-*t*-Bu groups with the appropriate intensities. The latter appears as a doublet owing to the four-bond ^{1}H–^{31}P coupling. ^{31}P NMR resonances are observed at δ 181 (**4a**) and 199 (**4b**) in THF-*d*$_8$ solution (cf. XP(μ-N-*t*-Bu)$_2$PX (δ 211, X = Cl; δ 224, X = Br)) (34). Surprisingly, the mass spectra of **4a** and **4b** show fragment ions corresponding to [M – Me]$^+$ and [M – N-*t*-Bu]$^+$ rather than [M – X]$^+$ implying a relatively strong covalent P–X (X = Cl, Br) bond. A molecular ion is observed for **4b**.

Table 5. Selected bond lengths (Å) and bond angles (deg) for **4b**.

Bond lengths (Å)		Bond angles (deg)	
Br(1)—P(1)	2.3047(11)	N(1)-P(1)-N(1)*	80.09(17)
P(1)—N(1)	1.688(3)	N(1)-P(1)-Br(1)	103.67(10)
N(1)—B(1)	1.440(4)	B(1)-P(1)-Br(1)	112.85(11)
N(1)—C(10)	1.470(5)	B(1)-N(1)-P(1)	90.41(19)
C(1)—B(1)	1.567(5)	B(1)-N(1)-C(10)	136.3(2)
		C(10)-N(1)-P(1)	130.6(2)
		N(1)*-B(1)-N(1)	97.9(3)
		N(1)-B(1)-C(1)	131.03(15)

Note: Symmetry transformations used to generate equivalent atoms *: *x*, –*y* + 1/2, *z*.

Fig. 4. ORTEP drawing of [PhB(μ-N-*t*-Bu)$_2$PN(H)-*t*-Bu] (**4c**) (30% probability ellipsoids).

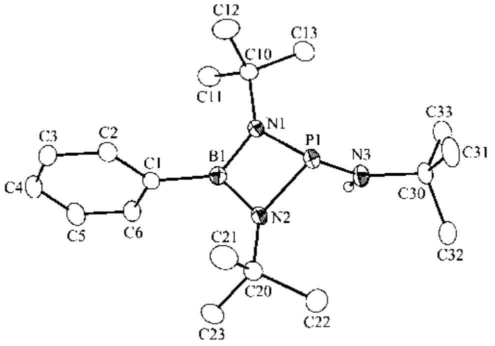

$$[3] \qquad 1/2\{Li_2[PhB(N\text{-}t\text{-}Bu)_2]\}_2 + PX_3 \rightarrow PhB(\mu\text{-}N\text{-}t\text{-}Bu)_2PX \qquad (X = Cl, Br)$$

The X-ray structure of **4b** is illustrated in Fig. 3 and selected bond lengths and bond angles are given in Table 5. The four-membered PNBN ring is slightly puckered (P(1)-N(1)-B(1)-N(1)* = 8.8(3)°) with symmetrically bridging N-*t*-Bu groups. The B–N bond lengths are in the typical range for phenylboraamidinate complexes (14) and the geometry at nitrogen is essentially planar. A search of the Cambridge Crystal Data Base revealed no structural information for cyclic P(III)–N compounds with exocyclic P–Br bonds. For example, the structure of the cyclodiphosph(III) azane BrP(μ-N-*t*-Bu)$_2$PBr is unknown (34). The P—N bond distance of 1.688(3) Å can be compared with values in the range 1.674(3)–1.689(9) Å for cyclodiphosph(III) azanes with Cl substituents attached to phosphorus (35, 36). The P—Br distance of 2.3047(11) Å is only slightly longer than the sum of the covalent radii for P and Br (2.24 Å) (27*b*), consistent with a strong covalent contribution to the P–Br bond.

The nucleophilic substitution reaction of **4a** with one equivalent of Li[N(H)-*t*-Bu] produced PhB(μ-N-*t*-Bu)$_2$PN(H)-*t*-Bu (**4c**) in ~80% yield. Amido derivative **4c** (see Table 6) was characterized by multinuclear (^{1}H, ^{13}C, ^{11}B, and ^{31}P) NMR and by X-ray crystallography (Fig. 4). The geometrical parameters of the phenylboraamidinate ligand in **4c** are similar to those discussed above for **4b**, although the four-membered ring is more puckered (torsion angle P(1)-N(1)-B(1)-N(2) = –12.50(13)°). The exocyclic P—N bond length of 1.6544(16) Å is ~0.1 Å shorter than

---

[9] The complex *t*-BuN(H)Sb(μ-N-*t*-Bu)$_2$TeCl$_2$ forms an extended structure involving weak Sb···Cl contacts rather than Te···Cl contacts (33).

Table 6. Selected bond lengths (Å) and bond angles (deg) for **4c**.

Bond lengths (Å)		Bond angles (deg)			
P(1)—N(1)	1.7395(14)	N(1)-P(1)-N(2)	77.37(7)	B(1)-N(2)-P(1)	90.81(11)
P(1)—N(2)	1.7452(14)	N(3)-P(1)-N(1)	105.28(7)	C(20)-N(2)-P(1)	128.08(11)
P(1)—N(3)	1.6544(16)	N(3)-P(1)-N(2)	106.66(7)	C(30)-N(3)-P(1)	129.85(13)
N(1)—B(1)	1.438(2)	B(1)-N(1)-P(1)	90.98(11)	C(30)-N(3)-H	112.0(14)
N(2)—B(1)	1.436(2)	B(1)-N(1)-C(10)	135.11(14)	P(1)-N(3)-H	118.1(14)
B(1)—C(1)	1.570(3)	C(10)-N(1)-P(1)	130.26(11)	N(2)-B(1)-N(1)	98.55(14)
		B(1)-N(2)-C(20)	132.45(14)	N(2)-B(1)-C(1)	131.32(16)
				N(1)-B(1)-C(1)	130.02(16)

Table 7. Selected bond lengths (Å) and bond angles (deg) for **5**.

Bond lengths (Å)		Bond angles (deg)			
P(1)—N(3)	1.6403(12)	N(3)-P(1)-N(1)	109.02(6)	C(30)-N(3)-P(1)	116.16(9)
P(1)—N(1)	1.7661(12)	N(3)-P(1)-N(2)	105.69(6)	C(30)-N(3)-Li(1)*	109.49(11)
P(1)—N(2)	1.8114(12)	N(1)-P(1)-N(2)	75.99(5)	P(1)-N(3)-Li(1)*	128.94(10)
N(1)—B(1)	1.4171(19)	B(1)-N(1)-C(10)	136.94(12)	C(30)-N(3)-Li(1)	136.83(11)
N(2)—B(1)	1.4762(19)	C(20)-N(2)-P(1)	121.40(9)	P(1)-N(3)-Li(1)	90.13(9)
N(2)—Li(1)	2.171(3)	B(1)-N(1)-P(1)	92.11(9)	Li(1)*-N(3)-Li(1)	70.38(12)
N(3)—Li(1)	2.084(3)	B(1)-N(2)-P(1)	88.41(9)	N(1)-B(1)-N(2)	99.13(12)
N(3)—Li(1)*	2.047(3)	C(10)-N(1)-P(1)	127.41(10)	N(1)-B(1)-C(1)	130.33(13)
C(1)—B(1)	1.573(2)	B(1)-N(2)-C(20)	126.64(11)	N(2)-B(1)-C(1)	129.94(13)
		B(1)-N(2)-Li(1)	113.87(11)	N(3)*-Li(1)-N(3)	109.62(12)
		C(20)-N(2)-Li(1)	112.92(11)	N(3)*-Li(1)-N(2)	136.97(14)
		P(1)-N(2)-Li(1)	83.10(8)	N(3)-Li(1)-N(2)	80.60(10)

Fig. 5. ORTEP drawing of $\{Li[PhB(\mu\text{-}N\text{-}t\text{-}Bu)_2PN\text{-}t\text{-}Bu]\}_2$ (**5**) (30% probability ellipsoids). Only the α-carbon atoms of *t*-Bu groups are shown. Starred atoms are related by the symmetry transformation: –*x* + 2, –*y*, –*z*.

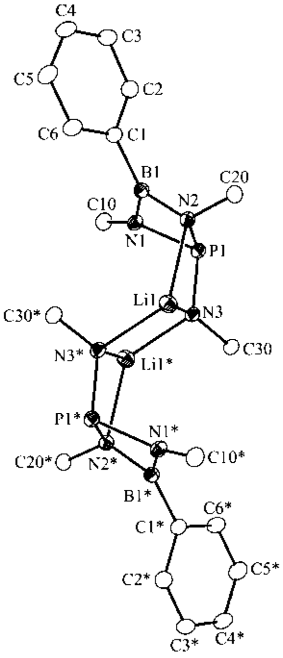

the mean endocyclic P–N bond distance and the geometry at N(3) is planar, suggesting a significant *p*π–*p*π interaction between N(3) and P(1).

The reaction of **4c** with one equivalent of *n*-BuLi produced the monolithium derivative $\{Li[Ph(\mu\text{-}N\text{-}t\text{-}Bu)_2PN\text{-}t\text{-}Bu]\}_2$ (**5**), which was shown by X-ray crystallography to be a centrosymmetric dimer (Fig. 5). The monomeric units in **5** are formed by *N*,*N'*-chelation of the $[PhB(\mu\text{-}N\text{-}t\text{-}Bu)_2N\text{-}t\text{-}Bu]^-$ anion to Li^+ through both the exocyclic and one of the endocyclic N atoms. As a result, one of the nitrogen atoms (N1) in the puckered PNBN ring (torsion angle P(1)-N(1)-B(1)-N(2) = 17.58(10)°) is three-coordinate, while the other (N2) is four-coordinate. As indicated in Table 7, this difference is reflected in an asymmetry in the B—N and P—N bond distances (1.4171(19) vs. 1.4762(19) Å and 1.7661(12) vs. 1.8114(12) Å, respectively). The relatively short P(1)—N(3) bond length (1.6403(12) Å) is comparable to the mean value of ~1.65 Å reported for the corresponding P—N bonds in $\{Li[P(N\text{-}t\text{-}Bu)_2]\}_4$ (37). The two monomeric units in **5** are linked by Li–N interactions to give a transoid ladder structure (38) with typical Li–N bond distances. The chelation of the $[PhB(\mu\text{-}N\text{-}t\text{-}Bu)_2PN\text{-}t\text{-}Bu]^-$ anion to Li^+ in **6** does not change the bond angles at the P(III) centre from those observed for **4c**.

The multinuclear (^1H, ^{13}C, ^7Li, ^{11}B, and ^{31}P) NMR data for **5** in THF-d_8 indicated the presence of two components, **5A** and **5B**, in solution in the approximate molar ratio 3:1. The relative intensities of the ^1H and ^{13}C NMR resonances for **5A** and **5B** both indicate C_6H_5, *endo*-*t*-Bu, and *exo*-*t*-Bu

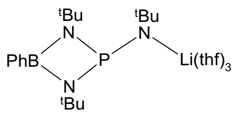

5A

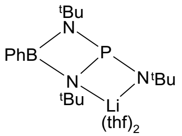

5B

groups in the ratio 1:2:1, consistent with the empirical formula Li[*t*-BuN(μ-N-*t*-Bu)$_2$BPh], in addition to a resonance for a three-coordinate boron atom. Both **5A** and **5B** exhibit singlets in the ^{31}P NMR spectra with chemical shifts of δ 129.9 and 68.1, respectively. It is well established that solvation of Li^+ centres in lithium derivatives of polyimido anions of *p*-block elements may lead to the disruption of polycyclic (cluster) structures or the stabilization of smaller aggregates (39). A pertinent example is the tetramer [Li{P(N-*t*-Bu)$_2$}]$_4$ (40), which forms the solvated dimer [(THF)Li{P(N-*t*-Bu)$_2$}]$_2$ in THF solution (41). Another, more dramatic, demonstration of this effect is the unraveling of the cyclic ladder structure of [Li$_2${C(N-*t*-Bu)$_3$}]$_2$ (42) upon solvation to give the open ladder [(THF)$_3$Li$_2${C(NPh)$_3$}]$_2$ (43). Although the imido (NR) groups are different in these two derivatives, the primary cause of the different structures is clearly the Li^+ centres. For **5**, in the presence of an excess of THF, the most likely solvated complexes are **5A** and **5B**. The former has equivalent endocyclic N-*t*-Bu environments, consistent with the ^{1}H NMR spectrum, while in **5B** this equivalence could arise as a result of exchange of the lithium centre between the two endocyclic nitrogen centres. Such fluxional processes in lithium derivatives of polyimido anions of *p*-block elements have low activation energies (39). The only significant change in the ^{31}P NMR spectrum over the temperature range 183–333 K was an adjustment of the relative amounts of **5A** and **5B** from 1.0:0.26 at 333 K to 1.0:0.65 at 183 K. In the ^{7}Li NMR spectrum, the singlet observed at δ 0.414 at 295 K was resolved into two resonances at δ 0.447 and –0.06 (1.0:0.57) at 233 K. In the ^{31}P NMR spectrum at 233 K the relative intensities of the two components were 1.0:0.61.

The origin of the difference of ~60 ppm in the ^{31}P NMR chemical shifts of **5A** and **5B** is not clear. Unfortunately, the NMR spectra of **5** in the non-coordinating solvent toluene are surprisingly complex and, consequently, do not shed further light on the solution species. The solid-state NMR spectrum of **5** show as a resonance at δ 113.35 with a shoulder at δ 111.28. The observation of a shoulder close to the main resonance is puzzling because **5** has an entrosymmetric structure. This may indicate the presence of a conformational isomer of **5** in the bulk sample that was used in the solid-state NMR experiment. For comparison, the solid-state ^{31}P NMR spectrum of **4c**, which is formed on hydrolysis of **5**, exhibits a singlet at δ 78.9.

In the light of recent work by Stahl et al. (42) on Ni(II) complexes of the mono-anion *cis*-[*t*-BuOP(μ-N-*t*-Bu)$_2$PN-*t*-Bu]$^-$, the ligand behaviour of [PhB(μ-N-*t*-Bu)$_2$PN-*t*-Bu]$^-$ towards transition metals offers the interesting possibility of the involvement of the P(III) centre in the coordination sphere.

Conclusions

Complexes **2**, **4a**, and **4b** are the first examples of boraamidinates-containing element–halide bonds, which provide an opportunity to explore the properties of the boraamidinate ligand via functionalization of the main-group element centre, e.g., in the formation of the monomeric tellurium imide **3** and the chelating P(III) monoanion **5**. An interesting feature of dilithiated boraamidinate complexes, which is not observed for the corresponding amidinates, is the formation of long-lived radicals upon oxidation. Detailed EPR studies will be necessary to characterize these radicals. This propensity for radical formation is likely to lead to interesting chemistry in future investigations of metal–halogen exchange reactions of lithium boraamidinates, especially for those metals which have two (or more) readily accessible oxidation states.

Acknowledgments

We thank the Natural Science and Engineering Research Council of Canada (NSERC) for financial support, Dr. R. McDonald (University of Alberta) for X-ray data collection of **1a** and **1b**, and Dr. M. Parvez for advice in the refinement of the X-ray structures.

References

1. For reviews, see (*a*) F.T. Edelmann. Coord. Chem. Rev. **137**, 403 (1994); (*b*) J. Barker and M. Kilner. Coord. Chem. Rev. **133**, 219 (1994).
2. (*a*) S. Dagorne, I.A. Guzei, M.P. Coles, and R.F. Jordan. J. Am. Chem. Soc. **122**, 274 (2000); (*b*) R. Duchateau, A. Meetsma, and J.H. Teuben. Chem. Commun. 223 (1996).
3. (*a*) E.A.C. Brussee, A. Meetsma, B. Hessen, and J.H. Teuben. Chem. Commun. 497 (2000); (*b*) E.A.C. Brussee, A. Meetsma, B. Hessen, and J.H. Teuben. Organometallics, **17**, 4090 (1998).
4. P. Blais, J.K. Brask, T. Chivers, C. Fedorchuk, and G. Schatte. ACS Symposium Series, in press (2002).
5. H. Heine, D. Fest, D. Stalke, C.D. Hebben, A. Meller, and G.M. Sheldrick. J. Chem. Soc. Chem. Commun. 742 (1990).
6. D. Fest, C.D. Habben, A. Meller, G.M. Sheldrick, D. Stalke, and F. Pauer. Chem. Ber. **123**, 703 (1990).
7. H.-J. Koch, H.W. Roesky, S. Besser, and R. Herbst-Irmer. Chem. Ber. **126**, 571 (1993).
8. C.D. Habben, A. Heine, G.M. Sheldrick, and D. Stalke. Z. Naturforsch. **47b**, 1367 (1992).
9. H. Fuβstetter and H. Nöth. Chem. Ber. **112**, 3672 (1979).
10. D. Gudat, E. Niecke, M. Nieger, and P. Paetzold. Chem. Ber. **121**, 565 (1988).
11. (*a*) C.D. Habben, A. Heine, G.M. Sheldrick, D. Stalke, M. Bühl, and P.v.R. Schleyer. Chem. Ber. **124**, 47 (1991); (*b*) C.D. Habben, R. Herbst-Irmer, and M. Noltemeyer. Z. Naturforsch. **46b**, 625 (1991).
12. W. Luthin, J.-G. Stratmann, G. Elter, A. Meller, A. Heine, and H. Gornitzka. Z. Anorg. Allg. Chem. **621**, 1995 (1995).
13. P. Paetzold, D. Hahnfeld, U. Englert, W. Wojnowski, B. Dreczewski, Z. Pawelec, and L. Walz. Chem. Ber. **125**, 1073 (1992).
14. T. Chivers, X. Gao, and M. Parvez. Angew. Chem. Int. Ed. Engl. **34**, 259 (1995).
15. J.K. Brask, T. Chivers, and G. Schatte. Chem. Commun. 1805 (2000).
16. D.W. Aubrey and M.F. Lappert. J. Chem. Soc. 2927 (1959).
17. N.D.R. Barnett, W. Clegg, L. Horsburgh, D.M. Lindsay, Q.-Y. Liu, F.M. Mackenzie, R.E. Mulvey, and P.G. Williard. Chem. Commun. 2321 (1996).
18. (*a*) SAINT V 5.0. Software for the CCD detector system. Bruker AXS, Inc., Madison, WI. 1998; (*b*) SADABS V. 2.01 (WindowsNT, Service Pack 6). Software for area-detector absorption and other corrections. Bruker AXS, Inc., Madison, WI. 2000; (*c*) HKL DENZO and SCALEPACK V1.96. Z. Otwinowski and W. Minor. *In* Processing of X-ray diffraction

data collected in oscillation mode: Methods in enzymology. Vol. 276. Macromolecular crystallography, Part A. *Edited by* C.W. Carter Jr. and R.M. Sweet. Academic Press, San Diego. 1997. pp. 307–326.

19. (*a*) G.M. Sheldrick. SHELXS-97. Program for the solution of crystal structures. University of Göttingen, Göttingen, Germany. 1997; (*b*) G.M. Sheldrick. SHELXL97–2. Program for the solution of crystal structures. University of Göttingen, Göttingen, Germany. 1997.
20. (*a*) A. Altomare, G. Cascarano, C. Giacovazzo, and A. Guagliardi. SIR-92. A package for crystal structure solution by refinement and direct methods. J. Appl. Crystallogr. **26**, 343 (1993); (*b*) A. Altomare, G. Cascarano, C. Giacovazzo, A. Guagliardi, A.G.G. Moliterni, M.C. Burla, G. Polidori, M. Camalli, and R. Spagna. SIR-97. A package for crystal structure solution and refinement by direct methods. Italy. 1997.
21. B. Eichorn, H. Nöth, and T. Seifert. Eur. J. Inorg. Chem. 2355 (1999).
22. (*a*) D.E. Wigley. Prog. Inorg. Chem. **42**, 239 (1994); (*b*) D.P. Smith, K.D. Allen, M.D. Carducci, and D.E. Wigley. Inorg. Chem. **31**, 1319 (1992).
23. R. Fleischer, S. Freitag, F. Pauer, and D. Stalke. Angew. Chem. Int. Ed. Engl. **35**, 204 (1996).
24. R. Fleischer, S. Freitag, and D. Stalke. J. Chem. Soc. Dalton Trans. 193 (1998).
25. J.K. Brask, T. Chivers, B. McGarvey, G. Schatte, R. Sung, and R.T. Boeré. Inorg. Chem. **37**, 4633 (1998).
26. T. Chivers, G.D. Enright, N. Sandblom, G. Schatte, and M. Parvez. Inorg. Chem. **38**, 5431 (1999).
27. (*a*) N.W. Alcock. Adv. Inorg. Chem. Radiochem. **15**, 1 (1972); (*b*) L. Pauling. The nature of the chemical bond. 3rd ed. Cornell University Press, Ithaca, NY. 1960. Chap. 7. p. 260.
28. H.W. Roesky, J. Münzenburg, R. Bohra, and M. Noltemeyer. J. Organomet. Chem. **418**, 339 (1991).
29. J. Münzenberg, H.W. Roesky, M. Noltemeyer, S. Besser, and R. Herbst-Imer. Z. Naturforsch. **48b**, 199 (1993).
30. H. Folkerts, K. Dehnicke, and J. Magull. Z. Naturforsch. **50b**, 573 (1995).
31. R. Boese, J. Dworak, A. Haas, and M. Pryka. Chem. Ber. **128**, 477 (1995).
32. J. Pietikäinen, R.S. Laitinen, and J. Valkonen. Acta. Chem. Scand. **53**, 963 (1999).
33. T. Chivers and G. Schatte. Inorg. Chem. **41**, 1002 (2002).
34. W. Jacksties, H. Nöth, and W. Storch. Chem. Ber. **118**, 2030 (1985).
35. K.W. Muir. J. Chem. Soc. Dalton Trans. 259 (1975).
36. L. Stahl. Coord. Chem Rev. **210**, 203 (2000), and refs. therein.
37. J.K. Brask, T. Chivers, M.L. Krahn, and M. Parvez. Inorg. Chem. **38**, 290 (1999).
38. A. Downard and T. Chivers. Eur. J. Inorg. Chem. 2193 (2001).
39. J.K. Brask and T. Chivers. Angew. Chem. Int. Ed. Engl. **40**, 3960 (2001).
40. J.K. Brask, T. Chivers, M.L. Krahn, and M. Parvez. Inorg. Chem. **38**, 290 (1999).
41. I. Schranz, L. Stahl, and R.J. Staples. Inorg. Chem. **37**, 1493 (1998).
42. T. Chivers, M. Parvez, and G. Schatte. J. Organomet. Chem. **550**, 213 (1998).
43. P.J. Bailey, A.J. Blake, M. Kryszczuk, S. Parsons, and D. Reed. J. Chem. Soc. Chem. Commun. 1647 (1995).
44. G.R. Lief, C.J. Carrow, L. Stahl, and R.J. Staples. Chem. Commun. 1562 (2001).